ELSEVIER

Biophysical Chemistry 120 (2006) 36 – 43

Biophysical Chemistry

http://www.elsevier.com/locate/biophyschem

Bead-like passage of chloride ions through ClC chloride channels

Atsushi Suenaga [a], Jay Z. Yeh [b], Makoto Taiji [a], Akira Toyama [c], Hideo Takeuchi [c], Mingyu Son [d], Kazuyoshi Takayama [d], Masatoshi Iwamoto [e], Ikuro Sato [f], Toshio Narahashi [b], Akihiko Konagaya [a], Kunihiko Goto [b,*]

[a] *Bioinformatics Group, RIKEN Genomic Sciences Center, 61-1 Ono, Tsurumi, Yokohama, Kanagawa 230-0046, Japan*
[b] *Department of Molecular Pharmacology and Biological Chemistry, Northwestern University Medical School, 303 East Chicago Avenue, Chicago, IL 60611-3008, USA*
[c] *Department of Pharmaceuticals, Graduate School of Pharmaceutical Sciences, Tohoku University, Aobayama, Sendai 980-8578, Japan*
[d] *Shock Wave Research Center, Institute of Fluid Science, Tohoku University, 2-1-1, Katahira, Sendai 980-8577, Japan*
[e] *Department of Applied Physics, Tohoku Gakuin University, 1-13-1, Tagajyo, Miyagi 985-8537, Japan*
[f] *Miyagi Prefecture Cancer Center, Natori, Miyagi, Japan*

Received 7 June 2005; received in revised form 27 September 2005; accepted 2 October 2005
Available online 9 November 2005

Abstract

The ClC chloride channels control the ionic composition of the cytoplasm and the volume of cells, and regulate electrical excitability. Recently, it has been proposed that prokaryotic ClC channels are H^+-Cl^- exchange transporter. Although X-ray and molecular dynamics (MD) studies of bacterial ClC channels have investigated the filter open–close and ion permeation mechanism of channels, details have remained unclear. We performed MD simulations of ClC channels involving H^+, Na^+, K^+, or H_3O^+ in the intracellular region to elucidate the open–close mechanism, and to clarify the role of H^+ ion an H^+-Cl^- exchange transporter. Our simulations revealed that H^+ and Na^+ caused channel opening and the passage of Cl^- ions. Na^+ induced a bead-like string of $Cl^--Na^+-Cl^--Na^+-Cl^-$ ions to form and permeate through ClC channels to the intracellular side with the widening of the channel pathway.

Keywords: ClC channels; Chloride channels; Molecular dynamics; Conformational change; Selectivity filter; Ion permeation

1. Introduction

The ClC chloride channels, which are ubiquitous channel proteins found in both prokaryotic and eukaryotic cells, play a crucial role in controlling the ionic composition of the cytoplasm and the volume of cells. In skeletal muscle, ClC chloride channels stabilize the resting membrane potential and regulate electrical excitability, thus, the ClC channels are the key enzyme in homeostasis of electrolytes [1–3]. Several structures of the ClC channels have been solved [4,5] and these structural analyses revealed that the ClC channels are homo-dimers in which each of the two identical subunits contains its own independently gated pore. The published X-ray structure of the bacterial ClC channel is a gate-closed state [4] whereas its mutation (E148A) is in a constitutively gate-open state [5]. Several theoretical studies [6–8] have attempted to clarify the molecular mechanism of ClC channels. Recently it has been proposed that prokaryotic ClC channels are H^+-Cl^- exchange transporters [9]. To survive in the acidic stomach, bacteria must extrude H^+ accumulated on the intracellular side in the extremely acidic environment. Bacteria use ClC channels as H^+-Cl^- exchange transporters in which intracellular H^+ moves toward the extracellular side, while extracellular Cl^- passes through to the intracellular side. Despite the availabilities of these experimental and theoretical data about the ClC channels, three fundamental questions remain; 1) what is the open–close mechanism of the gate? 2) how does the H^+ ion take part in the H^+-Cl^- transport mechanism? 3) why does each chain show independent conductance? To answer these questions, we performed molecular dynamics (MD) simulations of the ClC channels, and investigated the dynamics of not only H^+ but also other positive ions, Na^+, K^+ or H_3O^+ on the intracellular side.

* Corresponding author. Tel.: +1 312 503 6167; fax: +1 312 503 1700.
E-mail address: kunihikogoto@aol.com (K. Goto).

0301-4622/$ - see front matter © 2005 Elsevier B.V. All rights reserved.
doi:10.1016/j.bpc.2005.10.004

Only when H^+ or Na^+ resided in the intracellular interior of the channel protein, did we observe Cl^- passage to the intracellular side and the reverse movement of H^+ or Na^+ to the extracellular side. Both intracellular H^+ and Na^+ induced the Cl^- passage to the intracellular side, but intracellular Na^+ induced the formation of a bead-like string of Cl^-–Na^+–Cl^-–Na^+–Cl^- ions and the permeation of the bead-like string through ClC channels to the intracellular side. In this paper, we described Cl^- permeation which was driven mainly by intracellular Na^+.

2. Methods

2.1. Simulation methodology

MD simulation is a widely used and effective method to investigate the protein dynamics and its physical properties [10–13]. X-ray structures of ClC from *Salmonella serovar typhimurium* (StClC) (Protein Data Bank (PDB) ID: 1KPL), from *Escherichia coli* (EcClC)(PDB ID: 1KPK) [4], and those of mutant^{E148A} (1OTT) and mutant^{E148Q} (1OTU) from *E. coli* [5] were used as the initial structures for our simulations. The coordinates of the entire N-terminal segment for one of the two monomers (residues 12–32 in chain A) were absent in the X-ray structure, 1KPL. We have modeled this segment by duplicating it from the chain B and splicing it into chain A, because it would play an important role in its function. Each ClC was then placed in a DMPC membrane, which was modified with partial charge calculated using RHF/6–31*G single-point calculation with Gaussian 98 (Gaussian Inc.) and the restrained electrostatic potential method, and was solvated with TIP3P water molecules [14]. After the neutralization of the system by the random positioning of Na^+ and Cl^- (intracellular region for Na^+ and extracellular region for Cl^-), the solvent and counter ions except for ions in the pore were optimized by a 5000 steps of energy minimization while the position of ions in the pore and solute were fixed. Next, the solute and ions in the pore were optimized while the position of the counter ions and solvent atoms were kept frozen. All MD simulations were carried out using Amber ver. 7 [15] on personal computers (Pentium III 933 MHz × 32). The bond length involving hydrogen atoms was constrained to equilibrium length by the SHAKE method [16] and the time step was set at 1 fs. Amber parm96, a parameter set for molecular mechanical force fields used for simulations of biomolecules, was adopted [17]. The systems (including ~100,000 atoms) were heated to 300 K for 0.05 ns and equilibrated for 1.95 ns (total of 2.0 ns) in the NPT ensemble, with periodic boundary conditions and particle mesh Ewald method. The temperature and pressure were kept constant at 300 K (with a time constant of 1.0 ps) and 1 atm (with a relaxation time of 0.2 ps), respectively. In some simulations, during the equilibration, a voltage of 100 mV was applied across the pore (direction from the inside to the outside of the cell) to mimic the membrane potential and enhance the ion permeation [10].

2.2. Simulation systems

We examined the following systems (Fig. 1C): P0: 1KPL was made to hold Cl^- in the channel protein interior without 8 intracellular Na^+. P1: Eight Na^+ were located in the deep

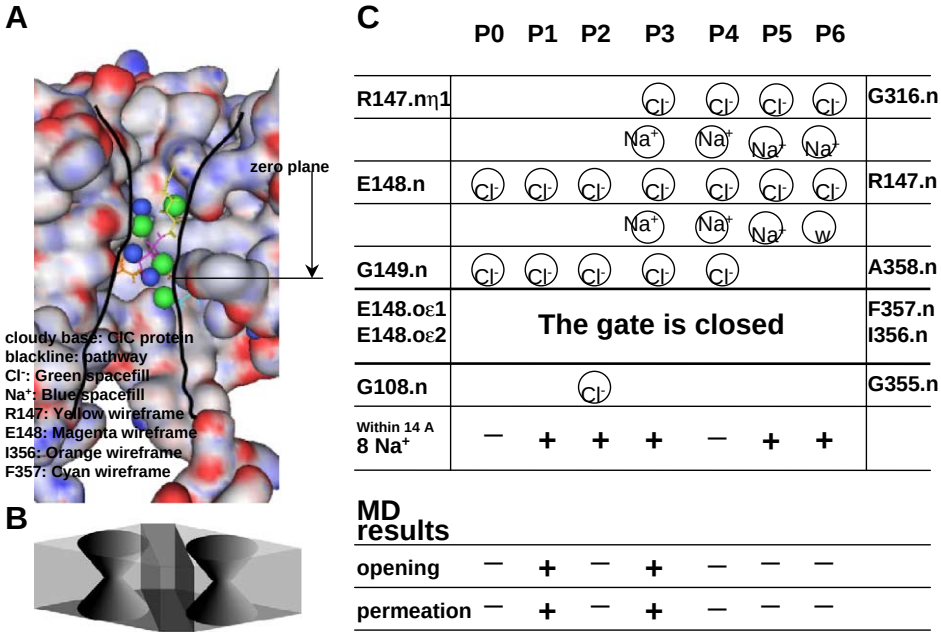

Fig. 1. Simulation systems. Channel pathway of the StClC (chain A). The ClC channel is represented by surface model which is colored according to electrostatic potential (the color is shaded red to blue corresponding to negatively to positively charge). Cl^- is shown light green spacefill model; Na^+, blue spacefill model; R147a, yellow wireframe; E148a, magenta wireframe; I356a, orange wireframe; F357a, cyan wireframe. The level of zero plane is shown (see Numerical calculation). B. Illustration of the ClC channel with the narrowest part (gate). The channel has two independent hourglass-shaped pores. C. The initial structure of each system is illustrated. The interface among E148.Oε1, E148.Oε2, I356.N, and F357.N forms the gate of the selectivity filter (neck of the hourglass-shaped pore). The gate is closed in initial structures. Other both side atoms are nitrogen atoms which bound with Cl^- ions in StClC channel simulations.

interior of the channel protein. P2: One Cl^- was sited on the intracellular side in the P1 structure. P3: Bead-like strand of Cl^-–Na^+–Cl^-–Na^+–Cl^- was placed on the Cl^- pathway with 8 intracellular Na^+. P4: Eight intracellular Na^+ in P3 were removed. P5: Cl^- of the gate side in P3 was removed. P6: One water molecule was substituted for Na^+ of the gate side in P5. For investigation of the effect of H^+, K^+, and H_3O^+ in the channels, we substituted Na^+ for H^+, K^+, or H_3O^+ in P1 and P3.

2.3. Numerical calculation

We calculated the channel volume using the MI2 program. The program calculates a volume of a closed space by filling 0.1 Å cube voxels (small boxes) [18] in the closed space and counts the number of voxels which enter in the closed space. We chose the cylinder-like structure consisting of N318.N level to G108.C level vertical to membrane in the channel pathway. For forming the cylinder-like wall consisting of about 60 atoms, we chose 23 atoms which reflected the cylinder volume and linked centers of neighboring atoms to make a closed space consisting of many triangular planes. We subtracted the van der Waals volume of atoms positioned at the triangular apex from the closed space. The closed space to be estimated consists of flat planes and many atomic dents (Fig. 3A).

The center between E148.Oε1 and E148.Oε2 and between I345.N and F346.N were calculated on both A and B chains. We divided the length between their centers on the same side into two and then found each center point (the center point of A chain, C; that of B chain, D). The plane consisting of two center points, C and D, and A421a.Cα were taken to be the zero plane, while the extracellular side from the zero plane was defined as the positive direction. The length of the line of a Cl^- vertical to the plane was found and the difference between their lengths was calculated as the locus of the Cl^-.

3. Results and discussion

3.1. Effect of intracellular Na^+ on Cl^- permeation

We loaded H^+, Na^+, K^+, or H_3O^+ in the intracellular side of the systems, as ClC channels did not show voltage-dependent gating [10], which is consistent with the findings that the electrophysiological analysis of bacterial ClC channels also showed no voltage-dependent gating [9]. First, we describe the effect of intracellular Na^+ on Cl^- permeation. In the case where there are 10 Na^+ between 25 Å (meaning the nearest position of the bulk medium to the gate) and 35 Å away from each (A or B chain) gate (Fig. 1A and B) (at the neck of the hourglass-shaped pore [5]), the opening of the gate did not occur (P0 in Fig. 1C). In the study of E148 protonation or deprotonation, NaCl electrolyte was used as the bulk medium, and Na^+ in the bulk medium did not induce Cl^- to pass through [8]. When 8 Na^+ were present within 14 Å from each gate in the initial structure, we could observe opening of the gate (gating) and passage of Cl^- (P1 in Fig. 1C). The condition, where 8 Na^+ were present within 14 Å in the medium of 0.001 N Na^+ (corresponds in that of H^+ of pH 3), was realized in about 300 ps (Supplementary material). On the intracellular side one Cl^- was loaded in the system which contained 8 intracellular Na^+ within 14 Å from the gate (P2 in Fig. 1C), and again no gating occurred. These findings would explain the electrophysiological finding that intracellular Cl^- inhibited Cl^- permeation [19]. After 1.9 ns simulation of P1, a bead-like strand consisting of Cl^-–Na^+–Cl^-–Na^+–Cl^-–two water molecules–Cl^-–one water molecule, was formed (Fig. 2Av; Table 1). Referring to the bead-like strand, we made an initial structure in which the bead-like structure resided in the extracellular side with intracellular 8 Na^+ and with the gate closed (P3 in Fig. 1C). In this system, the bead-like structure passed through the channel, showing transformation of the bead-like structure (Fig. 2B; Table 1). When there was no intracellular Na^+ of P3, this bead-like strand did not pass through (P4 in Fig. 1C). When one Cl^- nearest to the gate of selectivity filter was removed from P3, we could not see the gating and Cl^- permeation (P5 in Fig. 1C). This result that the nearest Cl^- was indispensable for Cl^- permeation would explain the finding that the ClC channel opening is promoted by its substrate, chloride [8,20]. When water is substituted for the Na^+ nearest to the selectivity filter gate, the Cl^- permeation did not occur (P6 in Fig. 1C). We observed Cl^- passage only when H^+ or Na^+ was loaded in P1 and P3, but not when K^+ or H_3O^+ was loaded.

3.2. Gating mechanism

In the condition of P1 and P3, the passage of Cl^- was observed. Fig. 2Ai, Aii, Bi, and Bii shows the gating mechanisms in an A channel of P1 conditioned StClC (2Ai and ii), and in a B channel of P3 conditioned StClC (2Bi and ii), respectively. First, some intracellular Na^+ bound with Oε1 and/or Oε2 of E148, and second, Cl^- bound with the Na^+ and with I356a.N (single letter of amino acid, sequence number, chain, and atom) and/or F357a.N, causing the jagged line, E148a.Oε1 (q) and/or E148a.Oε2 (r)–Na^+ (u)–Cl^- (a)–

Table 1
The coordination shell components of Figs. 2 and 3 snapshots

Molecule	Cl^-	Na^+	Main chain	Important	Important	Important
				Side chain	Oxygen	Nitrogen
Display	Spacefill	Spacefill	Fine line	Ball and stick	Ball and stick	Ball and stick
Color	Greenblue	Light blue	Grey	Grey	Magenta	Blue

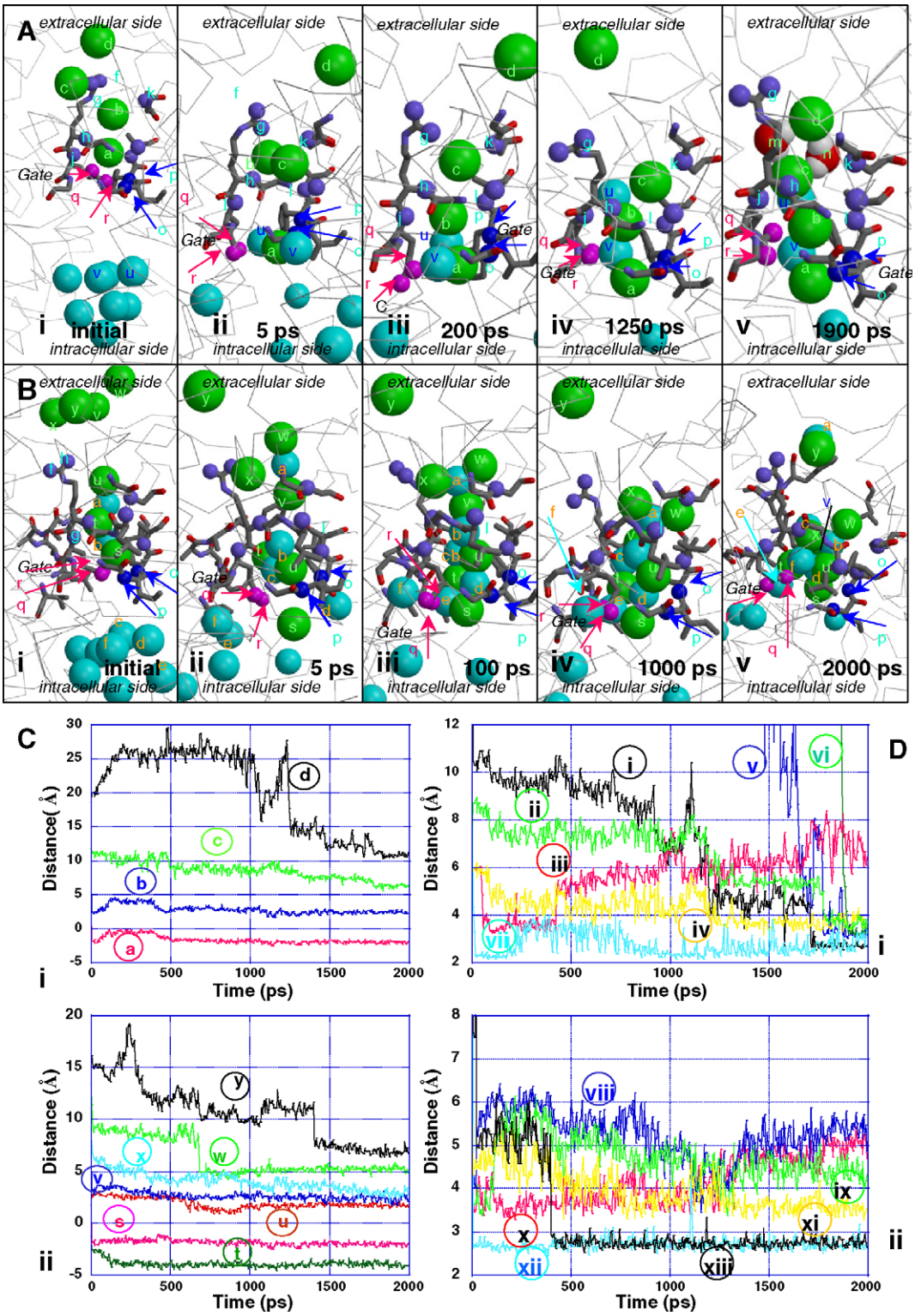

Fig. 2. Permeation dynamics in StClC A and B chains. A. Molecular dynamics series in P1 conditioned StClC A chain. i) Initial structure with closed gate. ii) 5 ps structure with opened gate. iii) 200 ps structure with opened gate. iv) 1250 ps structure with opened gate. v) 1900 ps structure with opened gate. Cl^- ions are shown by spacefill model (green) and labeled a to d (Table 1). Several protein atoms are labeled (R147a.Nη2, f; R147a.Nη1, g; R147a.N, h; L145a.N, i; E148a.N, j; G316a.N, k; A358a.N, l; I356a.N, o; F357a.N, p; E148a.Oε1, q; E148a.Oε2, r) and shown by balls. Two water molecules and three Na^+ ions are shown by spacefill model and labeled m, n, u and v, respectively. B. Molecular dynamics series in P3 conditioned StClC B chain. i) Initial structure with closed gate. ii) 5 ps structure with opened gate. iii) 100 ps structure with opened gate. iv) 1000 ps structure with opened gate. v) 2000 ps structure with opened gate. Six Cl^- ions are labeled s to x and six Na^+ ion are labeled a to f. C. Time courses in locus of Cl^- in chain A (i) and in chain B (ii) (see Numerical calculation). Each label of Cl^- corresponds to those in P1 (A) and P3 (B). D. Time courses of distances between Cl^- and protein atoms, water molecules or ions obtained from P1 simulation. i) Distances between Cl^- (labeled b in A) and Na^+ (labeled u in A), i; and E148.N, ii; and R147a.Nη1, iii; and R147a.N, iv; and water molecule (labeled m in A), v; and water molecule (labeled n in A), vi; and distance between Na^+ (labeled u in A) and E148.Oε2, vii. ii) Distances between Cl^- (labeled a in A) and E148.N, viii; and G149a.N, ix; and F357a.N, x; and I356a.N, xi; and Na^+ (labeled u in A), xii; and Na^+ (labeled v in A), xiii.

I356a.N (o) and/or F357a.N (p), to be formed and the gate consisting of E148a.Oε1 (q), E148a.Oε2 (r), I356a.N (o), and F357a.N (p) to open (Fig. 2A; Table 1). Thus, the 148 side chain acts as the gate to moved out, similar to findings observed by the X-ray structural analyses of wild type EcClC, mutant^{E148A}, and mutant^{E148Q} [5].

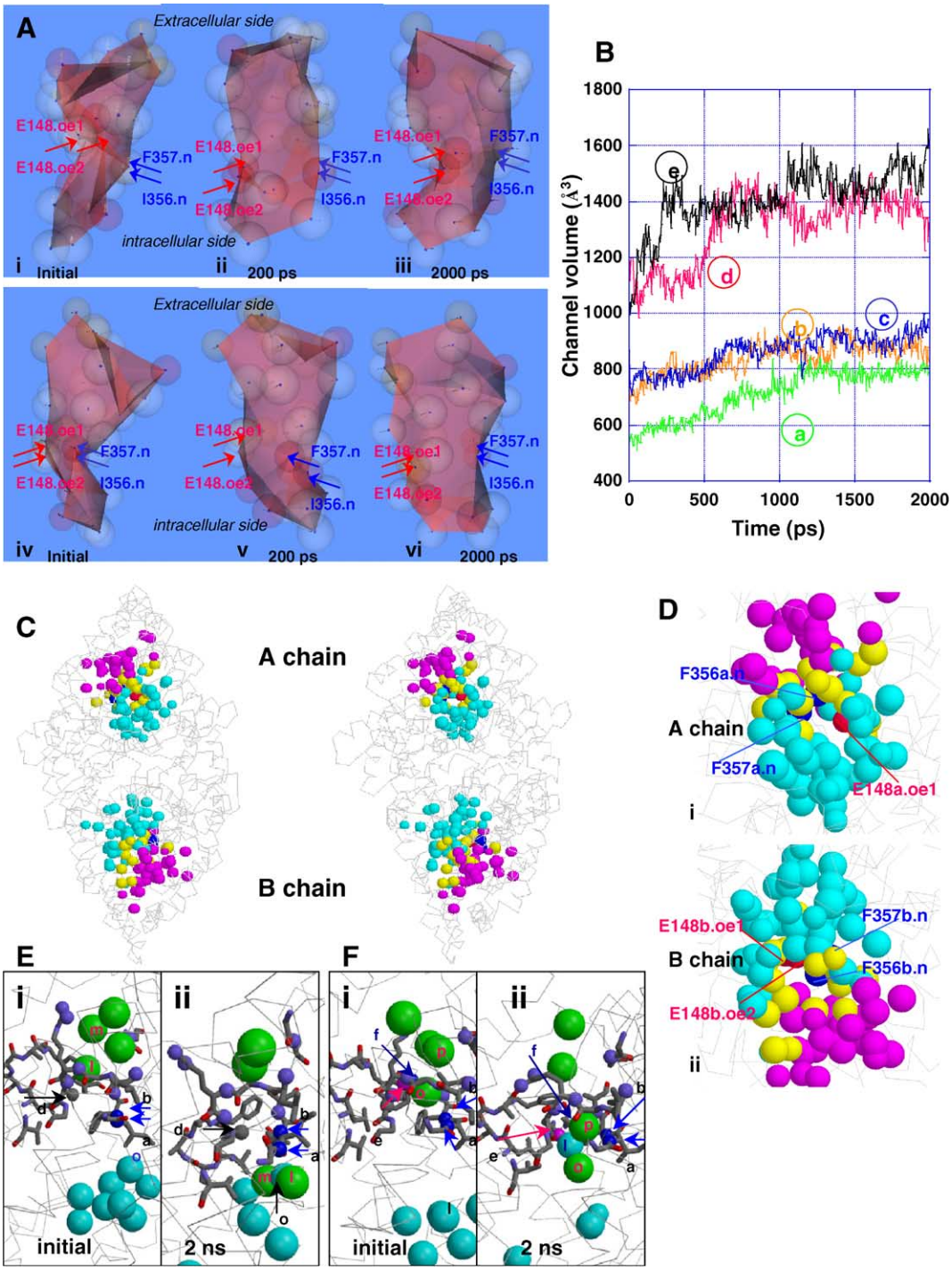

Fig. 3. Characterization of the ClC channel pathway. A. The P1 conditioned StClC A channel viewed three-dimensionally by using Nexternet Player (see Numerical calculation). The initial structure (i), 50 ps structure (ii), and 2000 ps structure (iii). The initial structure of the P1 conditioned EcClC (iv), 200 ps structure (v) and 2000 ps structure (vi). Note that the closed space is formed by linked centers of atoms and that the space does not represent the real space (see Numerical calculation). B. Volume changes of channel pathway. Time courses of channel volumes (see Numerical calculation). a) A StClC B channel (initial structure; P1). b) A StClC A channel (P1). c) An EcClC A channel (P1). d) Another StClC A channel (P3). e) An EcClC B channel (P3). C. Stereo views of StClC channel pathways in 100 ps structure. The view is from the extracellular side. Atoms proper for A chain underlining the channel pathway, cyan spacefill model; atoms proper for B chain pathway, magenta spacefill model; atoms common for A and B chain pathways, yellow spacefill model. D. i) StClC A chain pathway in 100 ps structure. ii) StClC B chain pathway. E. Mutant^{E148A} i) The initial structure with opened gate. ii) 2000 ps structure with opened gate. Two Cl^- ions passed through the channel (Table 1). I356a.N, a; F357a.N, b; A148a.Cb, d. F. Mutant^{E148Q}. i) The initial structure with the opened gate. ii) 2000 ps structure with the opened gate. Q148a.Oε1, e; Q148a.Nε2, f.

3.3. Formation and passage of bead-like string

During 2 ns in P1 conditioned StClC A chain, a bead-like strand, Cl^- (a)—Na^+ (v)—Cl^- (b)—Na^+ (u)—Cl^- (c)—two water molecules (m and n)—Cl^- (d), was gradually formed (Fig. 2A; Table 1). Also in other channels, StClC B, EcClC A, and EcClC B, the same mechanisms of the single-file formation in gating and bead-like formation in Cl^- permeation were found (not shown). This bead-like formation would be similar to the formation of K^+–water molecule–K^+–water molecule–water molecule–K^+, though the charge is reversed [21]. In a B channel of P3 conditioned StClC, the bead-like structure in the initial structure consisted of 3 Cl^- and 2 Na^+, and 200 ps later the structure became large to consist of 6 Cl^- and 5 Na^+. Furthermore, the enlarged bead-like structure was gradually transformed to make a larger mass, passing through the channel (Fig. 2Biii–v; Table 1). Though the number of the intracellular Na^+ gradually decreased over time, the intracellular Na^+ which were still present in the intracellular space would be an important cause in inducing the enlargement of the bead-like structure and the passing of the structure through the gate.

3.4. Interaction between protein and ion

To understand the relationship of ions and countercharged atoms of the protein in the bead-like formation, we analyzed the distance between Cl^- and nitrogen atoms of the channel protein, between Na^+ and Cl^-, between Cl^- and water molecules, and between Na^+ and oxygen atoms of the protein (Fig. 2D). Cl^- and Na^+ bound with each countercharged atom one after another. The shortest distance with vibration between each atom was almost the same, meaning that the shortest distance is the binding one. Since the binding force is inversely proportional to the square of the distance, the shorter the distance the larger the force. The strength order of binding forces is between Na^+ and protein oxygen atoms (2.3 ± 0.08 Å)>between Cl^- and Na^+ (2.7 ± 0.13 Å)>between Cl^- and water molecules (3.21 ± 0.16 Å)>between Cl^- and protein nitrogen atoms (3.6 ± 0.15 Å). Furthermore, in the protein interior, the electrostatic interaction becomes a stronger long-range force [22,23]. These findings would support phenomena that Na^+ first moved from the intracellular side to the extracellular side and Na^+ led the Cl^- permeation.

These findings indicate that intracellular Na^+ attracted extracellular Cl^- to the intracellular side and that Cl^- was caught on the way of the pathway by several protein nitrogen atoms. These phenomena of ion-counter charged atom interaction are general and suggest that these mechanisms should be included in models of the interaction of macromolecules, e.g., in the "rotation model" [24–31].

3.5. Widening of channel pathway

In the analysis of the bead-like formation, we found phenomena that the formation and the passage of bead-like structures induced the widening of not only the gate but also the channel pathway itself (Fig. 2A and B; Table 1). We observed changes of three dimensional structure of the channel pathway (Fig. 3A) and calculated volume changes in the channel pathway (Fig. 3B). Each channel showed gradual enlargement of the pathway volume. Both the volume itself and volume changes of P3 conditioned channels were larger than those of P1 conditioned channels (Fig. 3B).

3.6. Difference between underlining atoms in each chain

Furthermore, analyses of the volume changes in the channel pathway made us find the difference of atoms underlying channel pathway between A and B chain. The atoms underlying the StClC A channel pathway were largely different from ones of the StClC B chain, while 20 atoms consisting approximately 35% in each channel were common (Fig. 3C and 3D). The StClC A chain pathway resided nearer to the dimer interface than the B chain pathway (Fig. 3C and 3D). The EcClC A chain pathway was further from the dimer interface than the EcClC B chain pathway (not shown). Thus, even though Cl^- channels are homodimer [4,32], the atoms underlying the A chain pathway were different from those of the B chain pathway. ClC channels having two independent conductances for Cl^- [32–34] are partially explained by crystallographical findings that ClC channels consist of two independent pathways [4]. Our findings that the pathway structure of the A chain is different from that of the B chain would clearly explain the difference of transition time between the A and B chain in the MD simulation and two different conductances in ClC channels electrophysiologically [33]. In addition, these results for Na^+, bead-like passage of Cl^-, channel volume changes, and the difference of underlining atoms between the A and B chains, were similar to those for H^+ (Supplementary material).

3.7. Interaction of H^+, Na^+–Cl^-

We also analyzed Na^+ passage through the channel pathway from the intracellular to the extracellular side, opposite to Cl^- flow. We calculated how many more times the Na^+ passed through the gate from the intracellular to the extracellular side than the Cl^- went through the gate from the extracellular to the intracellular side. It was found that Na^+ went through by 1.31 ± 0.66 times than Cl^- did in the StClC A channel, 1.72 ± 0.85 times in the StClC B channel, 1.50 ± 0.50 times in EcClC A, and 1.25 ± 0.56 times in EcClC B channel. Intracellular Na^+ attracted Cl^-, and, after passing through the gate, Na^+ facilitated Cl^- permeation by formation of the bead-like structures (Fig. 2A and B). Thus, as a trigger of Cl^- passage, Na^+ would be as important as protons. Bacteria must survive in the extreme acidic, proton-rich, gastric juice, where bacteria must extrude protons accumulated during staying in the stomach using H^+–Cl^- exchange transporter of ClC channels [9]. However, bacteria must move through the stomach to proliferate in the small intestine and colon, where Na^+ is rich. To reach or stay near nutrient patches [35], the bacterial flagellar motor utilizes the electrochemical potential of Na^+ ions [36]. During the bacterial intensive movement, Na^+ is

accumulated on the intracellular side. The accumulated intracellular Na^+ would be the source of Na^+ as the trigger of Cl^- passage. Our findings would suggest that Na^+ are important for ClC channels as well as H^+. There was a report describing the relationship of Na^+ ions to function of ClC2 chloride channel [37], while there is no paper directly demonstrating Na^+–Cl^- exchange transporter in ClC channels electrophysiologically. Our simulation results suggest that it will be performed experimentally that some of ClC channels is Na^+–Cl^- exchange transporter.

3.8. Cl^- Passage in mutants

It has been proposed that Oε1 and Oε2 of E148 are important in Cl^- permeation [5]. The electrophysiological findings showed that in mutant^{E148A} and mutant^{E148Q} Cl^- passed through ClC channels but the passage of H^+ did not occur [9]. To estimate the further gating mechanism by Na^+ or H^+, we used mutant^{E148A}, and mutant^{E148Q} [5]. Two nanosecond MD analysis of these mutants showed that Cl^- passed through their ClC channels toward the intracellular side faster than through wild type ClC channels, while the passage of Na^+ or H^+ did not occur (Fig. 3E and F; Table 1; results of H^+ are not shown). These MD results of the faster Cl^- passage and the abolishment of H^+ were consistent with the above electrophysiological findings [9]. The gates of mutant^{E148A}, and mutant^{E148Q} stayed in the opened state during 2 ns, similar to the original crystal structures (Fig. 3Ei, Eii, Fi, and Fii; Table 1) [5]. In mutant^{E148A}, 2 Cl^- ions (l and m) passed through the mutant gate faster than through the wild type, because Cl^- ions would be attracted by intracellular Na^+ and 2 nitrogen atoms, I356.N (a) or F357.N (b), of the opened gate and then one Na^+ (o) bound them (Fig. 3E; Table 1). Because the jagged line of protein oxygen atom–Na^+–Cl^-–protein nitrogen atom shown in Gating mechanism was not formed in the mutant, Na^+ or H^+ could not pass through the gate. However, since the binding of Cl^- with protein nitrogen atom was generated and Na^+ or H^+ of inner side furthermore attracted Cl^-, Cl^- would pass through the gate. On the other hand, Na^+ and H^+ are repelled by the carbon atom of A148.cβ, not passing through the gate. In mutant^{E148Q}, 2 nitrogen atoms (a and b) and intracellular Na^+ would cause 2 Cl^- ions to move to the intracellular side, while one Na^+ (l) bound with Q148.Oε1 (e) and Cl^- ions (o and p) (Fig. 3F; Table 1). Only one oxygen, Q148.Oε1, (E148 possesses 2 oxygen atoms, Oε1 and Oε2) would cause Na^+ not to move to the extracellular side. However, what mechanisms prevent Na^+ or H^+ to pass through the gate are unknown. Henceforth, experiments using mutants would be a useful model to elucidate the molecular mechanisms of Cl^- channels.

4. Conclusions

1. Intracellular H^+ and Na^+ caused the channel to open and Cl^- ions to pass through in ClC channels.
2. Structure–function coupling occurred: A bead-like string of Cl^-–Na^+–Cl^-–Na^+–Cl^- ions formed by intracellular Na^+ permeated through ClC channels with the widening of the channel pathway.
3. Some of ClC channels might act as a Na^+–Cl^- exchange transporter.

Acknowledgements

We thank R. Yanai for technical assistance, H. Goto for illustration, H. Yoshikoshi and Y. Sasaki for encouragement, and N. Cook for the critical reading of the manuscript. This work was supported by the contracted research "Protein 3000 Project" by the Ministry of Education, Culture, Sports, Science and Technology of Japan (to A. S., M. T. and A. K.).

Appendix A. Supplementary data

Supplementary data associated with this article can be found in the online version at doi:10.1016/j.bpc.2005.10.004.

References

[1] R. Dutzler, The structural basis of ClC chloride channel function, Trends Neurosci. 27 (2004) 315–320.
[2] M. Pusch, Structural insights into chloride and proton-mediated gating of CLC chloride channels, Biochemistry 43 (2004) 1135–1144.
[3] T.J. Jentsch, V. Stein, F. Weinreich, A.A. Zdebik, Molecular structure and physiological function of chloride channels, Physiol. Rev. 82 (2002) 503–568.
[4] R. Dutzler, E.B. Campbell, M. Cadene, B.T. Chait, R. MacKinnon, X-ray structure of a ClC chloride channel at 3.0 Å reveals the molecular bases of anion selectivity, Nature 415 (2002) 287–294.
[5] R. Dutzler, E. Campbell, R. MacKinnon, Gating the selectivity filter in ClC chloride channels, Science 300 (2003) 108–112.
[6] J. Cohen, K. Schulten, Mechanism of anionic conduction across ClC, Biophys. J. 86 (2004) 836–845.
[7] B. Corry, M. O'Mara, S.-H. Chung, Conduction mechanisms of chloride ions in ClC-type channels, Biophys. J. 86 (2004) 846–860.
[8] L.D. Bostick, L.M. Berkowitz, Exterior site occupancy infers chloride-induced proton gating in a prokaryotic homolog of the ClC chloride channel, Biophys. J. 87 (2004) 1686–1696.
[9] A. Accardi, C. Miller, Secondary active transport mediated by a prokaryotic homologue of ClC Cl channels, Nature 427 (2004) 803–807.
[10] A. Suenaga, Y. Komeiji, M. Uebayashi, T. Meguro, M. Saito, I. Yamato, Computational observation of an ion permeation through a channel protein, Biosci. Rep. 18 (1998) 39–47.
[11] A. Suenaga, M. Hatakeyama, M. Ichikawa, X. Yu, N. Futatsugi, T. Narumi, K. Fukui, T. Terada, M. Taiji, M. Shirouzu, S. Yokoyama, A. Konagaya, Molecular dynamics, free energy, and SPR analyses of the interactions between the SH2 domain of Grb2 and ErbB phosphotyrosyl peptides, Biochemistry 42 (2003) 5195–5200.
[12] A. Suenaga, A.B. Kiyatkin, M. Hatakeyama, N. Futatsugi, N. Okimoto, H. Hirano, T. Narumi, A. Kawai, R. Susukita, T. Koishi, H. Furusawa, K. Yasuoka, N. Takada, Y. Ohno, M. Taiji, T. Ebisuzaki, J.B. Hoek, A. Konagaya, B.N. Kholodenko, Tyr-317 phosphorylation increases Shc structural rigidity and reduces coupling of domain motions remote from the phosphorylation site as reveled by molecular dynamics simulations, J. Biol. Chem. 279 (2004) 4657–4662.
[13] A. Suenaga, N. Takada, M. Hatakeyama, M. Ichikawa, X. Yu, K. Tomii, N. Okimoto, N. Futatsugi, T. Narumi, M. Shirouzu, S. Yokoyama, A. Konagaya, M. Taiji, Novel mechanism of interaction of p85 subunit of phosphatidylinositol 3-kinase and ErbB3 receptor-derived phosphotyrosyl peptides, J. Biol. Chem. 280 (2005) 1321–1326.
[14] W.L. Jorgensen, J. Chandrasekhar, J.D. Madura, R.W. Impey, M.L. Klein, Comparison of simple potential functions for simulating liquid water, J. Chem. Phys. 79 (1983) 926–935.

[15] D.A. Case, D.A. Pearlman, J.W. Caldwell, T.E. Cheatham III, J. Wang, W.S. Ross, C. Simmerling, T. Darden, K.M. Merz, R.V. Stanton, A. Cheng, J.J. Vincent, M. Crowley, V. Tsui, H. Gohlke, R. Radmer, Y. Duan, J. Pitera, I. Massova, G.L. Seibel, U.C. Singh, P. Weiner and P. A. Kollman, Amber version 7, University of California (San Francisco, 2002).
[16] J.-P. Ryckaert, G. Ciccotti, H.J.C. Berendsen, Numerical-integration of Cartesian equations of motion of a system with constraints-molecular dynamics of *n*-alkanes, J. Comput. Chem. 23 (1977) 327–341.
[17] P.A. Kollman, R. Dixon, W.D. Cornell, T. Fox, C. Chipot, A. Pohorille, The development/application of a 'minimalist' organic/biochemical molecular mechanics force field using a combination of ab initio calculations and experimental data, in: P. Wilkinson, P. Weiner, W.F. van Gunsteren (Eds.), Computer Simulation of Biological Systems, vol. 3, Elsevier, New York, 1997, pp. 83–96.
[18] J.S. Chen, W.-C. Lin, A new surface interpolation technique for reconstructing 3-D objects from serial cross-sections, 9th Internat, Conf. Pattern Recogn. (1988) 1100–1102.
[19] T.Y. Chen, C. Miller, Nonequilibrium gating and voltage dependence of the ClC-0 Cl-channel, J. Gen. Physiol. 108 (1996) 237–250.
[20] M. Pusch, U. Ludewig, A. Rehfeldt, T.J. Jentsch, Gating of the voltage-dependent chloride channel ClC-0 by the permeant anion, Nature 373 (1995) 527–531.
[21] S. Bernèche, B. Roux, Molecular dynamics of the KcsA K^+ channel in a bilayer membrane, Biophys. J. 78 (2000) 2900–2917.
[22] I.M. Klotz, Non-covalent bonds in protein structure, Brookhaven Sysp. Biol. 13 (1960) 25–48.
[23] G.C. Kresheck, I.M. Klotz, The thermodynamics of transfer of amides from an apolar to an aqueous solution, Biochemistry 8 (1969) 8–12.
[24] K. Goto, Transmembrane macromolecule rotation model-molecular hypothesis of membrane excitation, Tohoku J. Exp. Med. 139 (1983) 159–164.
[25] K. Goto, N. Sasano, Membrane macromolecular rotation model—unified molecular mechanism of secretion, Igakunoayumi 121 (1982) 201–203 (Japanese).
[26] K. Goto, The on–off mechanisms of the nicotinic acetylcholine receptor ion channel are performed by thermodynamic forces, J. Theor. Biol. 170 (1994) 267–272.
[27] K. Goto, Hydrophobic accessible surface areas are proportional to binding energies of serine protease–protein inhibitor complexes, Biochem. Biophys. Res. Commun. 206 (1995) 497–501.
[28] K. Goto, M. Iwamoto, Evidence of α-helix slidings during bacteriorhodopsin photocycle–energetics coupling, Tohoku J. Exp. Med. 182 (1997) 15–33.
[29] K. Goto, Rotation model—a molecular mechanism driven by hydrophobic and hydrophilic interactions, and underlying recognition and ion channels, Prog. Anesth. Mech. 5 (1998) 1–22.
[30] K. Goto, Rotation model—molecular hypothesis and predicting nAChR, anesthesia, enzyme catalysis, and immune signal transduction, J. Clin. Anesth. 23 (1999) 157–164 (Japanese).
[31] K. Goto, A. Toyama, H. Takeuchi, K. Takayama, T. Saito, M. Iwamoto, J.Z. Yeh, T. Narahashi, Ca^{++} binding sites in calmodulin and troponin C alter interhelical angle movements, FEBS Lett. 561 (2004) 51–57.
[32] R.E. Middleton, D.J. Pheasant, C. Miller, Homodimeric architecture of a ClC-type chloride ion channel, Nature 383 (1996) 337–340.
[33] C. Miller, Open-state substructure of single chloride channels from Toredo electroplax, Philos. Trans. R. Soc. Lond., B 299 (1982) 401–411.
[34] U. Ludewig, M. Pusch, T.J. Jentsch, Two physically distinct pores in the dimeric ClC-0 chloride channel, Nature 383 (1996) 340–343.
[35] S. Kojima, D.F. Blair, The bacterial flagellar motor: structure and function of a complex molecular machine, Int. Rev. Cyt. 233 (2004) 93–134.
[36] J. Manos, E. Artimovich, R. Belas, Enhanced motility of a *Proteus mirabilis* strain expressing hybrid FlaAB flagella, Microbiology 150 (2004) 1291–1299.
[37] J.K. Maskara, A. Rappert, K. Matthias, C. Steinhauser, A. Spat, H. Kettenman, Astrocytes from mouse brain slices express ClC-2-mediated Cl-currents regulated during development and after injury, Mol. Cell. Neurosci. 23 (2003) 521–530.